www.elsevier.nl/locate/jorganchem

Journal of Organometallic Chemistry 584 (1999) 366–375

Journal of Organometallic Chemistry

Divinyldisiloxane and divinylsilane complexes of rhodium(I)☆

Christine J. Cardin [a], Peter B. Hitchcock [b], Michael F. Lappert [b,*], Calum MacBeath [b], Nicholas J.W. Warhurst [b]

[a] *Reading University, Department of Chemistry, Reading RG6 6AD, UK*

[b] *University of Sussex, School of Chemistry, Physics & Environmental Science, The Chemistry Laboratory, Brighton, East Sussex BN1 9QJ, UK*

Received 22 January 1999; received in revised form 8 March 1999

Abstract

Reaction of the tetrakis(cyclooctene)rhodium(I) complex $[\{Rh(C_8H_{14}\text{-}c)_2(\mu\text{-}Cl)\}_2]$ with the appropriate divinyldisiloxane molecules $(ViSiR_2)_2O$ (R = Me or Ph) yields, by displacement of the cyclooctene ligands, the complexes $[\{Rh(ViSiR_2)_2O(\mu\text{-}Cl)\}_2]$ (R = Me (**1**) or Ph (**2**)). These react further with a tertiary phosphine PR'_3 to give *cis*-$[Rh\{(ViSiR_2)_2O\}(PR'_3)Cl]$ (R′ = Ph or C_6H_4Me-*p*). The complex *cis*-$[\{Rh(Vi_2SiMe_2)(\mu\text{-}Cl)\}_2]$ (**7**) was similarly prepared by the displacement of ethylene from $[\{Rh(C_2H_4)_2(\mu\text{-}Cl)\}_2]$ by the divinyldimethylsilane Vi_2SiMe_2. X-ray molecular structures of the crystalline complexes **1**, **2** and **7** show a distorted square planar Rh(I) environment, the CH_2=CH groups being orthogonal to this plane; **1** and **2** have the Rh–$(ViSiR_2)_2O$ metallacycle in the chair conformation, but differ in the nature of the central Rh(Cl)RhCl core, which is planar for **1** and puckered for **2**, but each of **1** and **2** is the *rac*-diastereoisomer, whereas **7** has the *meso*-configuration. In solution **1** and **2** exist as a mixture of isomers, probably the *rac*- and *meso*-pairs as established by multinuclear NMR spectral studies. A series of saturation transfer NMR spectroscopic experiments showed that the divinyldisiloxane ligands in $[\{Rh(ViSiPh_2)_2O(\mu\text{-}Cl)\}_2]$ underwent a dynamic process involving the dissociation, rotation and then reassociation of the vinyl groups.

Keywords: Tetramethyldivinyldisiloxane; Divinyldimethylsilane; Rhodium(I); Dynamic processes; Hydrosilylation

1. Introduction

Probably the most important catalyst for hydrosilylation is $H_2[PtCl_6]\cdot xH_2O$, Speier's catalyst, discovered in the mid-1950s [1]. It soon became apparent that for this to operate efficiently a 'solvent' was required in order to overcome the long and variable induction periods and the exothermic reactions. Such a solvent-modified system is the Karstedt catalyst [2], which incorporates the simplest divinyldisiloxane molecule $(CH_2$=$CHSiMe_2)_2O$ (≡LL). The generally accepted mechanism (Chalk–Harrod) of hydrosilylation postulated that the initiator was a Pt(0) species, probably formed by reduction of the chloroplatinic acid by the silane $HSiX_3$.

It was shown in 1987 that $H_2[PtCl_6]\cdot xH_2O$ with LL affords a solution **A** containing Pt(0) [3]. The evidence included (i) treatment of solution **A** with a tertiary phosphine led to recognisable Pt(0) species, e.g. $[Pt(PPh_3)_3]$ when PPh_3 was employed; (ii) reaction with PBu^t_3 gave the X-ray characterised platinum(0) complex $[Pt(LL)(PBu^t_3)]$ [3], and (iii) the $^{195}Pt\{^1H\}$-NMR spectrum of solution A showed a signal indicative of a platinum(0) complex.

Subsequently, a crystalline material was isolated from solution **A**, the X-ray structure of which established it to be the binuclear Pt(0) complex of formula $[\{Pt(LL)\}_2(\mu\text{-}LL)]$ [4]. This demonstrated inter alia that (i) the new ligand LL was capable of functioning not

☆ Dedicated to Professor Helmut Werner, as a mark of esteem and (by M.F. Lappert) of friendship.

* Corresponding author. Fax: +44-1273-677196.

E-mail address: m.f.lappert@sussex.ac.uk (M.F. Lappert)

0022-328X/99/$ - see front matter
PII: S0022-328X(99)00180-1

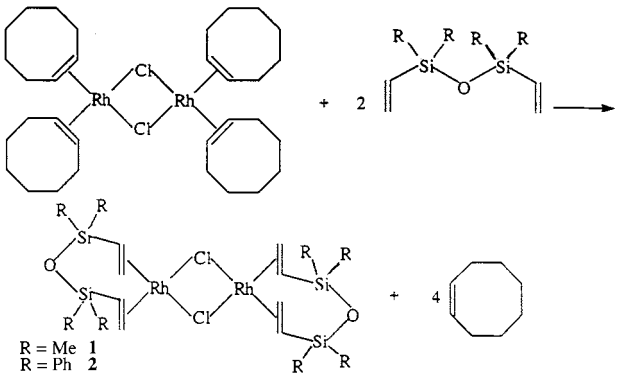

Scheme 1.

only in a chelating mode (i.e. as a terminal ligand), but it could also operate in a bridging fashion, and (ii) it was a reducing agent, converting a Pt(IV) chloride into a Pt(0) product.

We have shown that the bridging ligand in $[\{Pt(LL)\}_2(\mu\text{-LL})]$ was displaced by a mono-, bis- or tris(tertiary) phosphine to give, respectively, mono-, di- or trinuclear complexes featuring the di- and tridentate phosphines in unusual bridging modes [5,6]. The complex $[Pt(LL)PPh_3]$ has been prepared from $[Pt(C_2H_4)(PPh_3)_2]$ [7]. The ligand $(ViSiPh_2)_2O$ (L′L′) was introduced in the context of Ni(0) chemistry [6]. Thus, reduction of $[NiCl_2(PPh_3)_2]$ by zinc in the presence of LL or L′L′ afforded the X-ray-characterised $[\{Ni(\mu\text{-}L'L')(PPh_3)\}_2]$ or its LL analogue.

The reaction between nickel atoms and LL under metal vapour synthesis conditions yielded the tris(alkene)nickel(0) complex $[Ni(CH_2{=}CHSiMe_2OSiMe_2CH{=}CHSiMe_2)SiMe_2CH{=}CH_2)]$, [Ni(LL′L)] [8].

Two other types of Rh(I)–LL complexes have been reported: $[Rh(\eta^5\text{-}C_5H_5)(LL)]$ (R = H or Me) [9] and [Rh(acac)(LL)] [10].

An interesting feature of the divinyldisiloxane (LL) complexes is their stereochemical non-rigidity. Bassindale et al. reported that the variable temperature ^{1}H-NMR spectra of $[Pt(LL)(PBu^t_3)]$ could be interpreted in terms of an intramolecular exchange process involving the dissociation, rotation, then reassociation of the vinyl groups of the LL ligand [11]. A similar process, but in this case also involving rotation of an internal C=C group, was proposed for the dynamic behaviour observed in [Ni(LL′L)] [12].

2. Results and discussion

2.1. Synthesis and reactions of chloro(divinyldisiloxane)rhodium(I) complexes

Each of the binuclear Rh(I) complexes $[\{Rh(ViSiR_2)_2O(\mu\text{-Cl})\}_2]$ (R = Me (**1**) or Ph (**2**)) was synthesised by displacement of the four cyclooctene ligands from $[\{Rh(C_8H_{14})_2(\mu\text{-Cl})\}_2]$ by the appropriate divinyldisiloxane (Scheme 1). Compound **1** was not cleanly accessible by treatment of $RhCl_3{\cdot}xH_2O$ with $(ViMe_2Si)_2O$ in ethanol.

2.2. The X-ray molecular structures of $[\{Rh(ViSiR_2)_2O(\mu\text{-}Cl)\}_2]$ (R = Me (1) or Ph (2))

The X-ray molecular structure of crystalline **1** is illustrated in Fig. 1. Table 1 provides a list of bond lengths and angles. The molecule is dinuclear, having

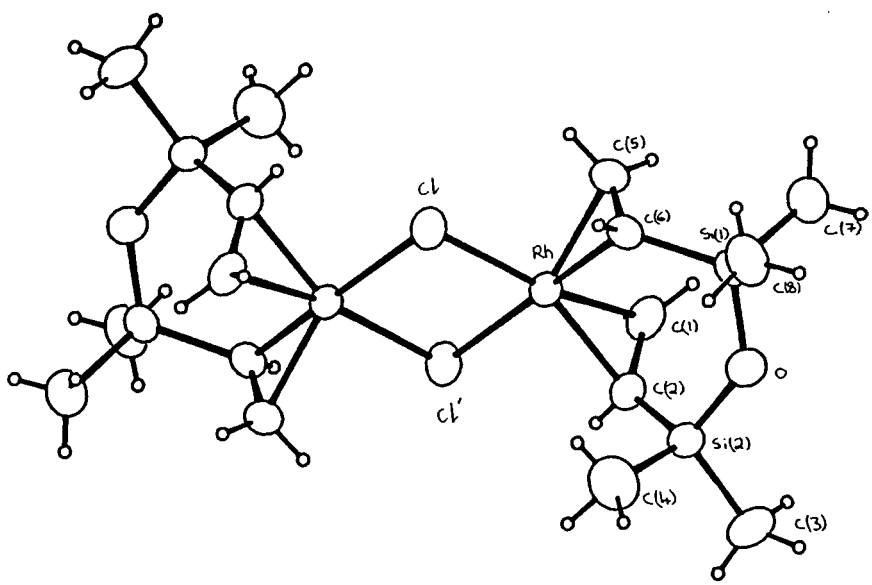

Fig. 1. The molecular structure of $[\{Rh(ViSiMe_2)_2O(\mu\text{-Cl})\}_2]$ (**1**). Selected bond lengths (Å) and angles (°): Rh(1)–C(1) = 2.141(5), Rh(1)–C(2) = 2.149(5), Rh(1)–C(5) = 2.113(6), Rh(1)–C(6) = 2.166(6); Rh(1)–Cl–Rh(2) = 96.78(5), Si(1)–O(1)–Si(2) = 133.0(3).

Table 1
Bond lengths (Å) and angles (°) for [{Rh(ViSiMe$_2$)$_2$O(μ-Cl)}$_2$] (**1**) [a]

Bond lengths (Å)			
Rh–Cl	2.392(2)	Rh–Cl′	2.403(1)
Rh–C(1)	2.141(5)	Rh–C(2)	2.149(5)
Rh–C(5)	2.113(6)	Rh–C(6)	2.166(6)
Si(1)–O	1.627(5)	Si(1)–C(2)	1.846(6)
Si(1)–C(3)	1.850(6)	Si(1)–C(4)	1.846(7)
Si(2)–O	1.629(4)	Si(2)–C(6)	1.880(6)
Si(2)–C(7)	1.848(7)	Si(2)–C(8)	1.843(7)
C(1)–C(2)	1.382(8)	C(5)–C(6)	1.387(8)
Bond angles (°)			
Cl–Rh–Cl′	83.22(5)	Cl–Rh–C(1)	95.4(2)
Cl–Rh–C(2)	86.2(2)	Cl–Rh–C(5)	149.4(2)
Cl–Rh–C(6)	168.6(1)	Cl′–Rh–C(1)	165.2(1)
Cl′–Rh–C(2)	155.9(2)	Cl′–Rh–C(5)	86.9(2)
Cl′–Rh–C(6)	89.5(1)	C(1)–Rh–C(2)	37.6(2)
C(1)–Rh–C(5)	87.0(2)	C(1)–Rh–C(6)	93.8(2)
C(2)–Rh–C(5)	112.4(2)	C(2)–Rh–C(6)	97.2(2)
C(5)–Rh–C(6)	37.8(2)	Rh–Cl–Rh	96.78(5)
O–Si(1)–C(2)	108.6(2)	O–Si(1)–C(3)	108.2(3)
O–Si(1)–C(4)	111.1(3)	C(2)–Si(1)–C(3)	108.8(3)
C(2)–Si(1)–C(4)	109.5(3)	C(3)–Si(1)–C(4)	110.6(3)
O–Si(2)–C(6)	111.4(2)	O–Si(2)–C(7)	109.1(3)
O–Si(2)–C(8)	108.4(3)	C(6)–Si(2)–C(7)	109.7(3)
C(6)–Si(2)–C(8)	108.6(3)	C(7)–Si(2)–C(8)	109.6(3)
Si(1)–0–Si(2)	133.0(3)	Rh–C(1)–C(2)	71.5(3)
Rh–C(2)–Si(1)	115.0(2)	Rh–C(2)–C(1)	70.9(3)
Si(1)–C(2)–C(1)	129.5(5)	Rh–C(5)–C(6)	73.2(3)
Rh–C(6)–Si(2)	124.7(2)	Rh–C(6)–C(5)	69.0(4)
Si(2)–C(6)–C(5)	121.9(4)		

[a] Symmetry element (′) x, y, z.

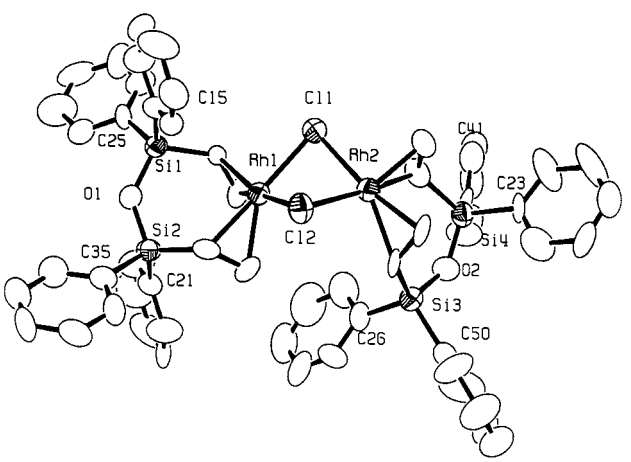

Fig. 2. The molecular structure of [{Rh(ViSiPh$_2$)$_2$O(μ-Cl)}$_2$] (**2**). Selected bond lengths (Å) and angles (°): Rh(1)–C(1) = 2.183(11), Rh–C(2) = 2.124(12), Rh–C(3) = 2.149(10), Rh–C(4) = 2.128(11); Rh(1)–Cl(1)–Rh(2) = 81.25(9), Si(1)–O(1)–Si(2) = 134.7(6).

an inversion centre at the mid-point of the central Rh(Cl)(Rh)Cl rhombus, the angle at Rh being narrower at Rh, average 83.2(1)°, than that at Cl, average 96.8(1)°. The local geometry at each four-coordinate rhodium is thus distorted square planar: $RhCl_2M_2$, M being the mid-point of each orthogonal vinyl group of the chelating LL ligand. It is noteworthy that crystalline **1** is diastereospecifically the *rac*- (rather than *meso*-, or a mixture of the two) isomer.

The X-ray molecular structure of the dinuclear crystalline **2**, having a similarly distorted square planar arrangement about each four-coordinate rhodium, is shown in Fig. 2, bond lengths and angles being presented in Table 2. Like **1**, crystalline **2** is the *rac*-diastereoisomer, but unlike in **1** the Rh(Cl)(Rh)Cl core in **2** is puckered rather than (as in **1**) planar, the angles at Rh and Cl being similar, an average of 82.1(2) and 81.4(2)°, respectively.

The metallacyclic RhMSiOSi'M' fragment in each of **1** and **2** is in the chair conformation, as was previously found for the chelated PtMSiOSi'M' fragments in the various Pt(0)–LL complexes [3–6]. Some of the average key bond distances and Si–O–Si′ angles in **1** and **2** are identical and unexceptional: Rh–M 2.02(1)°, C=C 1.38(1) Å, Rh–Cl 2.39(2) Å and Si–O–Si 133.0(3)°; cf. Rh–Cl 2.38(1) Å in [{Rh(μ-Cl)(COD)}$_2$] [13] and for [{Pt(LL)}$_2$(μ-LL)]: Pt–M 2.07(2) Å, C=C 1.39(3) Å and Si–O–Si 134.7(8)° for the chelating Pt(LL) [4a].

*2.3. NMR spectroscopic studies on the chloro(divinyldisiloxane)rhodium(I) complexes **1** and **6***

The ^{1}H-NMR spectrum of [{Rh(LL)(μ-Cl)}$_2$] (**1**) in [$^2H_8$]-toluene at 297 K showed broad signals due to the vinylic (δ 2.8–4.5) and methyl (δ −0.5 to +0.5) protons, which sharpened upon cooling to 253 K (for data see Section 3.1). At 253 K, two pairs of methyl signals (equatorial Me_e and axial Me_a) in a ratio of 2:1 were observed, indicating the presence of two isomers. The vinylic protons at δ 2.8–4.5 were shifted by ca. 2 ppm to a lower frequency relative to the values in the free ligand LL (δ 5.8–6.8). Following Cramer's description for 'inner' (H^3 in **I**) and 'outer' (H^1 and H^2 in **I**) hydrogens [14], H^1 and H^2 are assigned to the signals at the higher frequency, at δ 3.95 and 4.54, respectively; in the light of the former showing the greater coupling constant to H^3. Neither the geminal (^{2}H/^{3}H) nor ^{1}H–^{103}Rh coupling was observed.

The ^{13}C{^{1}H}-NMR spectrum of **1** in [$^2H_8$]-toluene at 303 K (see Section 3.1) also provided evidence for the existence of two isomers in solution. The CH^2H^3 signal for each isomer is believed to be at the higher frequency than that of CH^1, a result confirmed by recording the proton-coupled spectrum. The ^{29}Si{^{1}H}-NMR spectrum of **1** in [$^2H_8$]-toluene at 253 K showed two sharp signals in a ratio of ca. 2:1 (see Section 3.1).

We conclude that the isomers of **1** in solution are probably the *rac*- (the major, as in the crystal) and *meso*-diastereoisomers, also by analogy with the conclusion drawn from a more detailed study on the [{Rh(LL)(μ-Cl)}$_2$] system (vide infra).

Table 2
Selected bond lengths (Å) and angles (°) for **2**

Bond lengths (Å)	
Rh(1)–C(2)	2.125(12)
Rh(1)–C(4)	2.128(11)
Rh(1)–C(3)	2.149(10)
Rh(1)–C(1)	2.183(11)
Rh(1)–Cl(1)	2.381(3)
Rh(1)–Cl(2)	2.387(3)
Rh(1)–Rh(2)	3.1063(14)
Rh(2)–C(6)	2.090(12)
Rh(2)–C(7)	2.150(11)
Rh(2)–C(8)	2.172(11)
Rh(2)–C(5)	2.188(12)
Rh(2)–Cl(2)	2.379(3)
Rh(2)–Cl(1)	2.390(3)
Si(2)–O(1)	1.622(8)
Si(2)–C(1)	1.818(14)
Si(2)–C(35)	1.831(12)
Si(2)–C(21)	1.873(12)
Si(3)–O(2)	1.637(9)
Si(3)–C(26)	1.823(13)
Si(3)–C(7)	1.846(12)
Si(3)–C(50)	1.862(13)
Si(1)–O(1)	1.634(8)
Si(1)–C(15)	1.824(12)
Si(1)–C(3)	1.842(10)
Si(1)–C(25)	1.870(12)
Si(4)–O(2)	1.627(8)
Si(4)–C(5)	1.850(15)
Si(4)–C(23)	1.851(12)
Si(4)–C(41)	1.881(13)
Bond angles (°)	
C(2)–Rh(1)–C(4)	86.3(5)
C(2)–Rh(1)–C(3)	113.8(5)
C(4)–Rh(1)–C(3)	38.0(4)
C(2)–Rh(1)–C(1)	38.3(5)
C(4)–Rh(1)–C(1)	93.1(5)
C(3)–Rh(1)–C(1)	98.7(4)
C(2)–Rh(1)–Cl(1)	146.7(4)
C(4)–Rh(1)–Cl(1)	95.7(4)
C(3)–Rh(1)–Cl(1)	85.7(3)
C(1)–Rh(1)–Cl(1)	170.2(3)
C(2)–Rh(1)–Cl(2)	86.8(4)
C(4)–Rh(1)–Cl(2)	165.4(4)
C(3)–Rh(1)–Cl(2)	155.3(3)
C(1)–Rh(1)–Cl(2)	89.4(3)
Cl(1)–Rh(1)–Cl(2)	83.18(11)
C(2)–Rh(1)–Rh(2)	101.2(4)
C(4)–Rh(1)–Rh(2)	120.0(4)
C(3)–Rh(1)–Rh(2)	132.3(3)
C(1)–Rh(1)–Rh(2)	128.3(3)
Cl(1)–Rh(1)–Rh(2)	49.50(8)
Cl(2)–Rh(1)–Rh(2)	49.20(8)
C(6)–Rh(2)–C(7)	112.0(5)
C(6)–Rh(2)–C(8)	86.9(5)
C(7)–Rh(2)–C(8)	38.9(5)
C(6)–Rh(2)–C(5)	37.4(4)
C(7)–Rh(2)–C(5)	96.7(5)
C(8)–Rh(2)–C(5)	94.7(5)
C(6)–Rh(2)–Cl(2)	147.8(3)
C(7)–Rh(2)–Cl(2)	87.4(3)
C(8)–Rh(2)–Cl(2)	94.2(4)
C(5)–Rh(2)–Cl(2)	170.1(3)
C(6)–Rh(2)–Cl(1)	87.2(4)
C(7)–Rh(2)–Cl(1)	155.4(3)
C(8)–Rh(2)–Cl(1)	164.3(4)
C(5)–Rh(2)–Cl(1)	89.5(4)
Cl(2)–Rh(2)–Cl(1)	83.17(12)
C(6)–Rh(2)–Rh(1)	135.6(4)
C(7)–Rh(2)–Rh(1)	108.4(3)
C(8)–Rh(2)–Rh(1)	137.4(4)
C(5)–Rh(2)–Rh(1)	120.7(3)
Cl(2)–Rh(2)–Rh(1)	49.45(8)
Cl(1)–Rh(2)–Rh(1)	49.25(8)
Rh(1)–Cl(1)–Rh(2)	81.25(9)

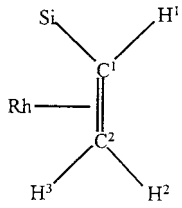

I

A series of variable temperature ^{1}H-NMR spectra of **2** in [$^{2}H_8$]-toluene is illustrated in Fig. 3 for the vinyl region, and indicates that this is a dynamic system containing two isomers; the low temperature (241 K) limiting spectral data are recorded in Section 3.2 together with the assignments. Coupling to ^{103}Rh, as for **1**, was not observed. The vinyl groups gave rise, as for **1**, to two doublets and a doublet of doublets. At 241 K, in addition to the three major signals for the vinyl protons, there were also smaller signals of similar multiplicity, attributed to the minor diastereoisomers. At 378 K, only one set of peaks was present, indicating that the two isomers were undergoing fast exchange; the coalescence temperature was in the range of 304–308 K. Unlike in **1**, the ^{29}Si{^{1}H} spectrum revealed only a single signal, albeit broad, at δ 5.3.

The result of a saturation transfer experiment, carried out on the phenyl region of the ^{1}H-NMR spectrum of **2** in $^{2}H_8$-toluene at 353 K, is shown in Fig. 4. Upon irradiation at the frequency of the signal at δ 8.25, there was a reduction in the intensity of the peak at δ 7.89; this indicates that at this temperature the *gem*-phenyl groups of the two isomers **2a** and **2b** (i.e. the same proton occurs at δ 8.25 in one isomer and δ 7.89 in the other) were exchanging.

The proposed mechanism for this dynamic process is shown in Scheme 2. The *rac*- and *meso*-diastereoisomers are represented by **2a** and **2b**, respectively. The scheme shows how dissociation, then rotation of the vinyl group of one of the divinyldisiloxane ligands can cause the interconversion of the isomers. The intermediate **8** has the L′L′ ligand in a staggered (or 'twisted chair') conformation similar to the intermediates observed in the dynamic processes involving [Ni(LL′L)] [12] and [Rh(η^5-C_5H_5)(LL)] [9].

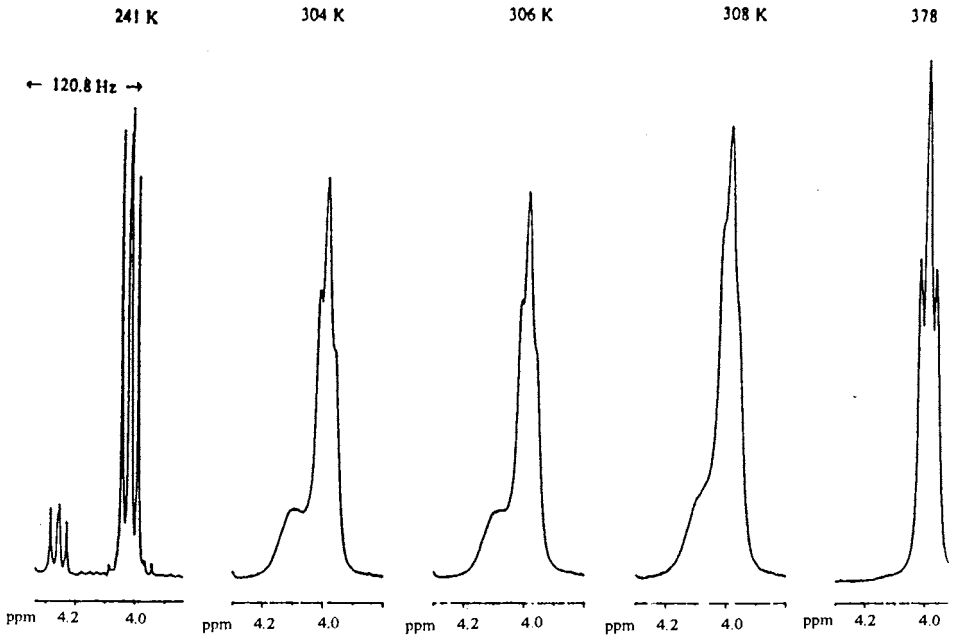

Fig. 3. Variable temperature ^{1}H-NMR spectral studies on [{Rh{ViSiPh$_2$)$_2$O(μ-Cl)] (**2**) recorded in [$^2H_8$] toluene, 500 MHz.

To establish whether the process was proceeding via the dissociation of the vinyl groups, a small amount of the free L′L′ ligand $(CH_2{=}CHSiPh_2)_2O$ was added to the sample and the frequency of a signal due to bound vinyl protons (in this case the doublet at δ 4.40 due to the methylene proton H^2 (see **I**) *cis* to the methine proton H^1) was irradiated. At 353 K, there was no reduction in the intensity of any signal. However, at 400 K, there was a reduction in the intensity of the peaks at δ 6.40 due to the equivalent protons of the free ligand (Fig. 5). These results show that the process involves dissociation of the vinyl groups, which at elevated temperatures can be intermolecular.

The ^{1}H and ^{13}C{^{1}H}-NMR spectral data for the complexes [Rh(LL)(PR′$_3$)] R = Ph (**3**), C_6H_{11}-*c* (**4**) or C_6H_4Me-*p* (**5**) and [Rh(L′L′)P(C_6H_4Me-*p*)$_3$] (**6**) are shown in Sections 3.3, 3.4, 3.5 and 3.6, and ^{29}Si{^{1}H} also for **5** (Section 3.5) and **6**.

The ^{31}P{^{1}H}-NMR spectra for each of the complexes **3**–**6** showed a doublet, with coupling between the rhodium and phosphorus atoms in the range of 176–186 Hz. These values are closer to those for a *trans*-alkene(tertiary phosphine)rhodium(I) complex than its *cis* analogue.

The ^{1}H and ^{13}C{^{1}H}-NMR spectra for each of these complexes displayed only one vinyl environment; no ^{1}H–^{103}Rh coupling was observed. These results suggest that the chelating vinylsiloxane ligand in complexes **3**–**6** is fluxional, exhibiting dynamic behaviour similar to that of the COD ligand in [Rh(COD)(PPh$_3$)Cl] [15].

2.4. Synthesis, NMR spectra and X-ray molecular structure of [{Rh(Vi$_2$SiMe$_2$)(μ-Cl)}$_2$] (7)

We have previously reported the synthesis of the binuclear divinyldimethylsilane(triphenylphosphine)-nickel(0) complex [{Ni(μ-Vi$_2$SiMe$_2$)(PPh$_3$)}$_2$] (**8**) [6], which featured the divinylsilane in a bridging mode **II**. We now describe the orange–red crystalline divinylsilane complex [{Rh(Vi$_2$SiMe$_2$)(μ-Cl)}$_2$] (**7**), prepared by the displacement of ethylene ligands from [{Rh-(CH$_2$=CH$_2$)$_2$)(μ-Cl)}$_2$], Eq. (1). Complex **7** was air-sensitive, both in the solid state and in solution; it was readily soluble in both aliphatic and aromatic hydrocarbons.

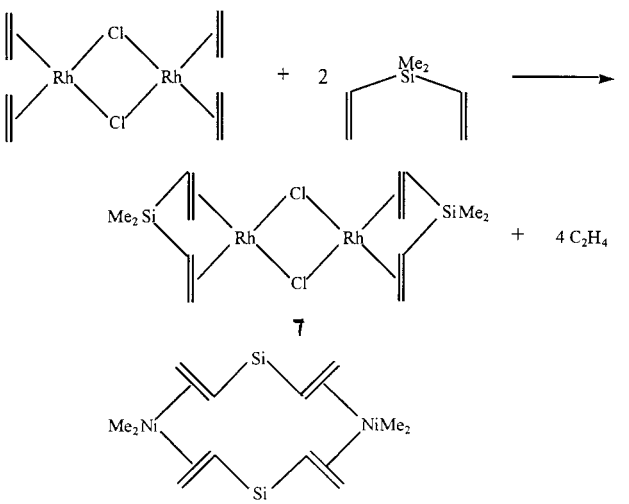

7

II

(1)

Multinuclear NMR spectra of **7** in [$^2H_8$]-toluene are recorded in Section 3.7. In the ^{1}H-NMR spectrum separate signals were shown for the methyl protons, consistent with those arising from axial (Me_a) and equatorial (Me_e) substituents at silicon in the chelating ligand. The assignments, shown in **III**, were made on the basis of a pair of nOe experiments, which showed that Me_a gave rise to a stronger nOe for H^3 than H^1, whereas Me_e produced a strong nOe upon H^1. Unlike the ambient temperature spectrum of **2**, no minor signals were observed for **7**, which only appeared upon cooling; as for **2**, these are attributed to the two diastereoisomers. The coalescence temperature was in the range of 239–243 K; similar features were observed in the $^{13}C\{^1H\}$-NMR spectra, showing twice the number of peaks at 200 K than at 313 K. Only C-2 showed coupling to ^{103}Rh. The $^{29}Si\{^1H\}$-NMR spectral chemical shift at δ −4.4 is 7.5 ppm to a higher frequency compared with that in the free silane Vi_2SiMe_2.

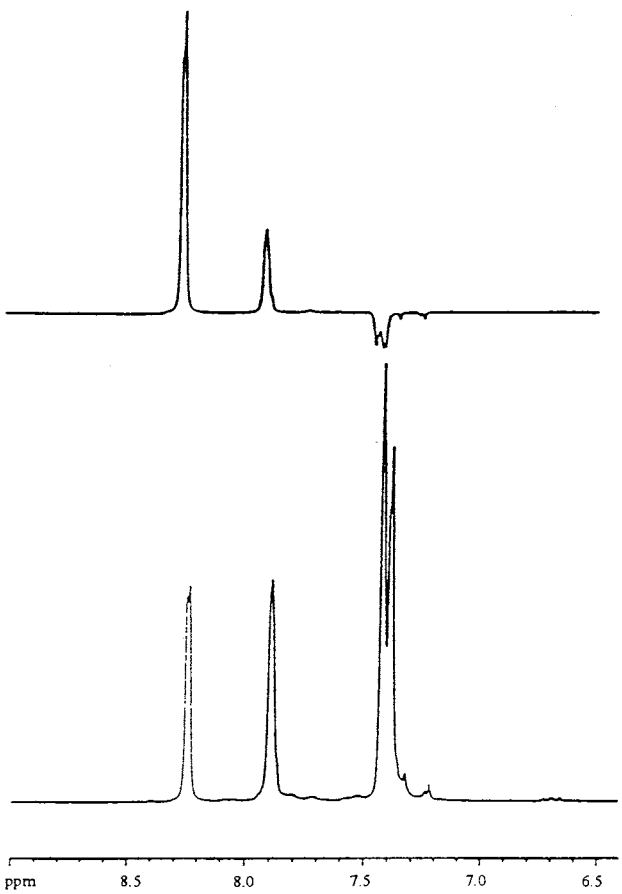

Fig. 4. Saturation transfer studies on [{Rh(ViSiPh$_2$)$_2$O(μ-Cl)}$_2$] (**2**) (phenyl region) recorded in [$^2H_8$]-toluene at 353 K, 500 MHz. The upper spectrum results from subtracting the effect of irradiating the frequency of the peak at δ 8.25 from the normal spectrum at this temperature (shown in the lower spectrum).

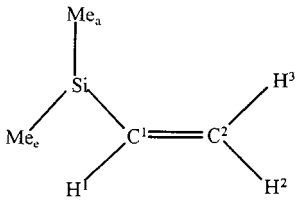

III

The X-ray molecular structure of crystalline **7** is shown in Fig. 6; structural parameters are listed in Table 3. As for **1** and **2**, there is a distorted square planar geometry about each rhodium atom, with the vinyl groups orthogonal to the plane. The square planar geometry is likely to place less strain on the molecule than the trigonal planar geometry for Ni(0) in [{Ni(μ-Vi$_2$SiMe$_2$)(PPh$_3$)}$_2$] (**8**), enabling the divinylsilane molecule in **7** to act as a chelating ligand. The average bond angle of 93.8°, formed by the centroid M of each of the two vinyl groups and the silicon atom, is significantly smaller than the 117.0° observed in [{Ni(μ-Vi$_2$SiMe$_2$)(PPh$_3$)}$_2$] [6]. Crystalline **7** is the *meso*-diastereoisomer, a result which contrasts with those for **1** and **2**. As for **2**, the Rh(Cl)(Rh)Cl core in **7** is puckered, the angle at rhodium being slightly wider (average 85.7(1)°) than that at Cl, average 82.1(3)°. Other geometric parameters are unexceptional.

3. Experimental

3.1. Synthesis of [{Rh(ViSiMe$_2$)$_2$O(μ-Cl)}$_2$] (1)

Tetramethyldivinyldisiloxane (5 ml) was added to a rapidly stirring yellow suspension of [{Rh(C$_8$H$_{14}$)$_2$(μ-Cl)}$_2$] (1230 mg, 1.7 mmol) in toluene (15 ml) at 25°C to give a deep red solution. The reaction mixture was stirred for 1 h at 25°C. The volatiles were removed under reduced pressure. The residual red solid was dissolved in toluene (10 ml) and filtered through Celite (2 × 2.5 ml), then washed with toluene (2 × 5 ml). The combined filtrate and washings were concentrated under reduced pressure to ca. 2 ml, yielding the red precipitate of **1** (900 mg, 1.39 mmol, 82%), which was filtered, washed with pentane (2 × 3 ml) and dried in vacuo. Red crystals (m.p. 130–131°C) suitable for X-ray diffraction were obtained by dissolving the red solid in the minimum amount of toluene and cooling the solution to 0°C.

Anal. Found: C, 29.3; H, 5.0. $C_{54}H_{48}Cl_2O_2Rh_2Si_4$. Calc. C, 29.6; H, 5.3%. ^{1}H-NMR (C_7D_8, 253 K, 360 MHz) major isomer [minor isomer]: δ 0.03 [−0.01] (s, Me_e, 12H), 0.54 [0.43] (s, Me_a, 12H), 2.98 [2.94] (d, H^3, 4H), 3.59 [3.63] (dd, H^1, 4H), 4.54 [4.44] (d, H^2, 4H), $^3J(^1H^1-^1H^2) = 11.9$ Hz, $^3J(^1H^1-^1H^3) = 14.5$ Hz.

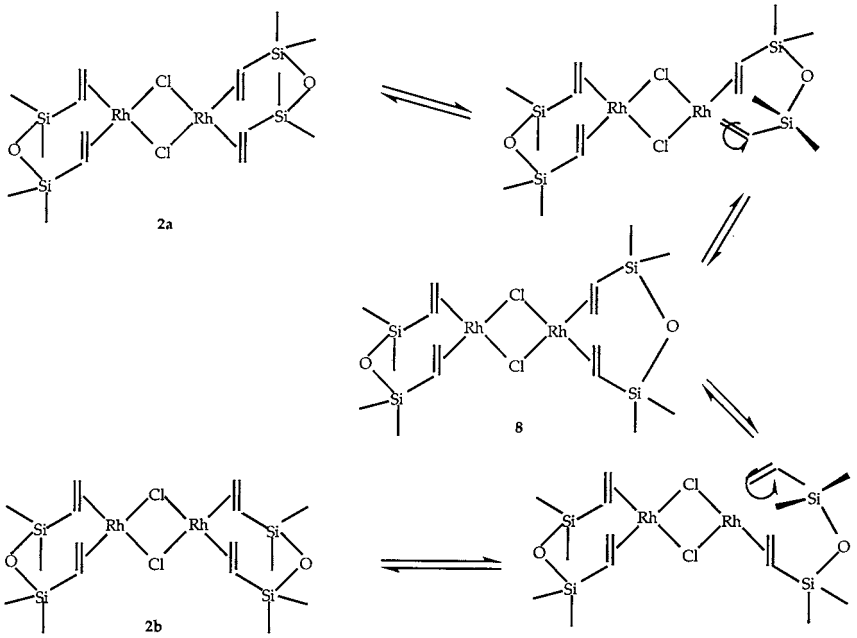

Scheme 2.

$^{13}C\{^1H\}$-NMR (C_7D_8, 303 K, 90 MHz): δ −0.9–1.9 (s, Me_e), 1.5 [0.5] (s, Me_a), 60.0 [62.4] (d, C^1), 66.7 (d, C^2), $^1J(^{13}C^1-^{103}Rh) = 13.7$ Hz, $^1J(^{13}C^2-^{103}Rh) = 12.5$ Hz. $^{29}Si\{^1H\}$-NMR (C_7D_8, 253 K, 72 MHz): δ 5.3 (s).

3.2. Synthesis of [{Rh(ViSiPh$_2$)$_2$O(μ-Cl)}] (2)

Tetraphenyldivinyldisiloxane (0.20 g, 0.47 mmol) was added to a rapidly stirred suspension of [{Rh(C_8H_{14}-*c*)$_2$(μ-Cl)}$_2$] (0.14 g, 0.21 mmol) in toluene (5 ml). The reaction mixture was stirred for 1 h, the colour changing from yellow–orange to deep red. The mixture was filtered through Celite and then washed with toluene; the solvent and cyclooctene were removed from the filtrate under reduced pressure to yield a deep red oil which upon addition of diethyl ether (2 ml) precipitated deep red crystals of **2** (0. 18 g, 0.16 mmol), m.p. 117–119°C. Crystals suitable for X-ray diffraction were obtained by dissolving the solid in the minimum amount of toluene followed by adding an equal amount of diethyl ether; these solvents were allowed to diffuse during 72 h at 25°C.

Anal. Found: C, 56.7; H, 4.3. $C_{54}H_{48}Cl_2O_2Rh_2Si_4$. Calc. C, 58.7; H, 4.6%. ^1H-NMR (C_7D_8, 241 K, 500 MHz) major isomer [minor isomer]: δ 2.98 [3.30] (d, H^3, 4H), 4.03 [4.26] (dd, H^1, 4H), 4.40 (d, H^2, 4H), 7.04–7.98 (m, Ph, 40H), $^3J(^1H^1-^1H^2) = 12.2$ Hz, $^3J(^1H^1-^1H^3) = 15.6$ Hz. $^{13}C\{^1H\}$-NMR (C_7D_8, 298 K, 125.8 MHz): δ 58.9 (s, C^1), 71.0 (d, C^2), 127.6–136.6 (m, Ph), $^1J(^{13}C^2-^{103}Rh) = 10.4$ Hz. $^{29}Si\{^1H\}$-NMR (C_7D_8, 298 K, 99.4 MHz): δ −12.1 [−12.15] (s).

3.3. Synthesis of [Rh{(ViSiMe$_2$)$_2$O}(PPh$_3$)Cl] (3)

Triphenylphosphine (170 mg, 0.64 mmol) was added to a rapidly stirring solution of **1** (190 mg, 0.29 mmol) in toluene (8 ml) at 25°C. The resultant solution was concentrated to ca. 2 ml under reduced pressure. The addition of pentane (4 ml) caused precipitation of the yellow solid **3** (250 mg, 0.41 mmol, 74%), which was filtered, washed with pentane (2 × 3

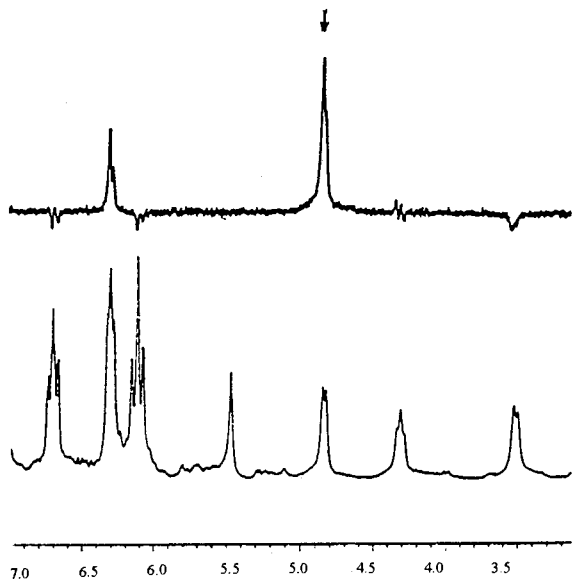

Fig. 5. Saturation transfer studies on [{Rh(ViSiPh$_2$)$_2$O(μ-Cl)}$_2$] (**2**) (phenyl region) recorded in [$^2H_8$]-toluene at 413 K, 500 MHz. The upper spectrum results from subtracting the effect of irradiating the frequency of the peak at δ 4.40 from the normal spectrum at this temperature (shown in the lower spectrum).

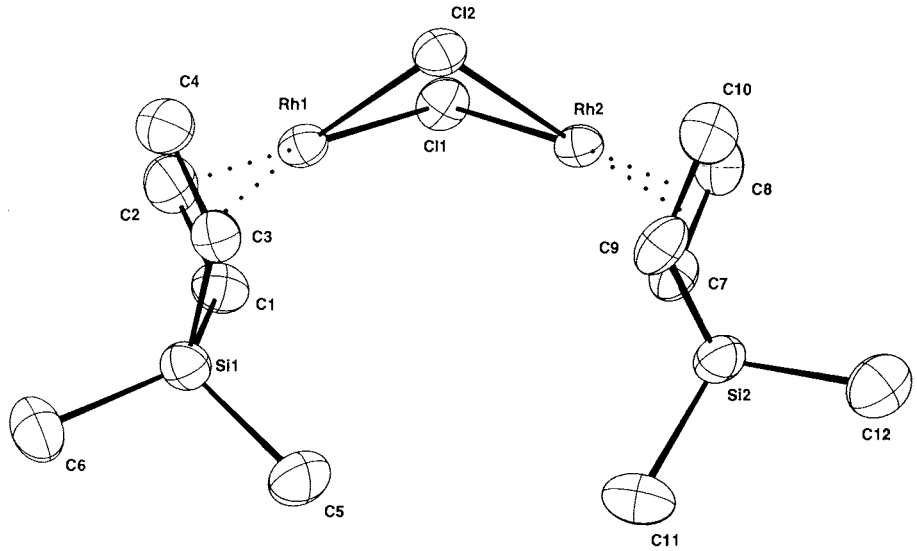

Fig. 6. The molecular structure of [{Rh(Vi$_2$SiMe$_2$)(μ-Cl)}$_2$] (**7**). Selected bond lengths (Å) and angles (°): Rh(1)–C(1) = 2.146(8), Rh–C(2) = 2.134(10), Rh–C(3) = 2.141(8), Rh–C(4) = 2.135(9); Rh(1)–Cl(1)–Rh(2) = 82.03(7).

ml) and dried in vacuo. Yellow crystals, m.p. 174–176°C, were obtained by dissolving the yellow solid in the minimum amount of toluene and cooling the solution to −30°C.

Anal. Found: C, 52.0; H, 8.1. $C_{26}H_{33}ClOPRhSi_2$. Calc. C, 51.6; H, 8.9%. ^{1}H-NMR (C_7D_8, 241 K, 500 MHz): δ 0.26 (s, Me$_e$, 6H), 0.50 (s, Me$_a$, 6H), 2.27 (m, H^1, 2H), 2.56 (d, H^2, 2H), 3.95 (d, H^3, 2H), 6.8–7.8 (m, Ph, 15H), $^3J(^1H^1-^1H^2) = 10.4$ Hz, $^3J(^1H^1-^1H^3) = 14.2$ Hz. ^{13}C{^{1}H}-NMR (C_7D_8, 298 K, 125.8 MHz): δ 3.3 (s, Me$_e$), 3.6 (s, Me$_a$), 53.5 (d, C^1), 54.0 (d, C^2), 125–136 (m, Ph), $^1J(^{13}C^1-^{103}Rh) = 16.7$ Hz, $^1J(^{13}C_2$-$^{103}Rh) =$ 14.7 Hz. ^{31}P{^{1}H}-NMR (C_7D_8, 303 K, 32 MHz): δ 51.2 (d), $^1J(^{31}P-^{103}Rh) = 186$ Hz.

3.4. Synthesis of [Rh{(ViSiMe$_2$)$_2$O}(PCy$_3$)Cl] (4)

The yellow complex **4** (200 mg, 0.40 mmol, 70%), m.p. 126–128°C, was prepared in a similar manner to **3**, except that dichloromethane was used as the reaction solvent instead of toluene.

Anal. Found: C, 54.2; H, 5.7. $C_{26}H_{33}ClOPRhSi_2$. Calc. C, 53.2; H, 5.7%. ^{1}H-NMR (CD_2Cl_2, 241 K, 500 MHz): δ −0.03 (s, Me$_e$, 6H), 0.45 (s, Me$_a$, 6H), 1.5–2.6 (m, Cy, 33H), 2.23 (d, H^2, 2H), 2.49 (dd, H^1, 2H), 2.87 (d, H^3, 2H), $^3J(^1H^1-^1H^2) = 10.6$ Hz, $^3J(^1H^1-^1H^3) = 14.0$ Hz. ^{31}P{^{1}H}-NMR (C_7D_8, 303 K, 32 MHz): δ 48.9 (d), $^1J(^{31}P-^{103}Rh) = 176$ Hz.

3.5. Synthesis of [Rh{(ViSiMe$_2$)$_2$O}P(C$_6$H$_4$Me-p)$_3$Cl] (5)

The yellow–orange crystalline complex **5** (0.32 g, 0.50 mmol, 73%), m.p. 179–181°C, was prepared in a similar manner to **3**.

Anal. Found: C, 54.9; H, 6.1. $C_{29}H_{39}ClOPRhSi_2$. Calc. C, 55.4; H, 6.3%. ^{1}H-NMR (C_7D_8, 298 K, 500 MHz): δ 0.29 (s, Me$_e$, 6H), 0.58 (s, Me$_a$, 6H), 1.95 (s, MeC$_6$H$_4$, 9H), 2.24 (m, H^1, 2H), 2.68 (d, H^2, 2H), 4.01 (d, H^3, 2H), 6.80–7.85 (m, MeC$_6$H$_4$, 12H), $^3J(^1H^1-^1H^2) = 12.0$ Hz, $^3J(^1H^1$-$^1H^3) = 14.1$ Hz. ^{13}C{^{1}H}-NMR (C_7D_8, 298 K, 125.8 MHz): δ 3.0 (s, Me$_e$), 3.7 (s, Me$_a$), 21.1 (s, MeC$_6$H$_4$), 53.0 (d, C^1), 54.2 (d, C^2), 128.9–139.9 (m, MeC$_6$H$_4$), $^1J(^{13}C^1-^{103}Rh) = 17.0$ Hz, $^1J(^{13}C^2-^{103}Rh) = 13.2$ Hz. ^{29}Si{^{1}H}-NMR (C_7D_8, 298 K, 99.4 MHz) δ 5.7 (dd), $^3J(^{29}Si-^{31}P) = 1.7$ Hz, $^2J(^{29}Si-^{103}Rh) = 1.9$ Hz. ^{31}P{^{1}H}-NMR (C_7D_8, 298 K, 101 MHz): δ 52.4 (d), $^1J(^{31}P-^{103}Rh) = 182$ Hz.

3.6. Synthesis of [Rh(ViSiPh$_2$)$_2$O}P(C$_6$H$_4$Me-p)$_3$Cl] (6)

The yellow crystalline complex **6** (0.12 g, 0.14 mmol, 78%), m.p. 194–196°C, was prepared in a similar manner to **3**.

Anal. Found: C, 67.0; H, 5.3. $C_{49}H_{47}ClOPRhSi_2$. Calc. C, 67.1; H, 5.4%. ^{1}H-NMR (C_7D_8, 298 K, 500 MHz): δ 2.02 (s, MeC$_6$H$_4$, 9H), 2.81 (d, H^2, 2H), 3.16 (dd, H^1, 2H), 4.12 (d, H^3, 2H), 6.75–7.82 (m, MeC$_6$H$_4$, 12H), 7.01–8.15 (m, Ph, 20H), $^3J(^1H^1-^1H^2) = 10.6$ Hz, $^3J(^1H^1-^1H^3) = 13.9$ Hz. ^{13}C{^{1}H}-NMR (C_7D_8, 298 K, 125.8 MHz): δ 21.3 (s, MeC$_6$H$_4$), 57.8 (d, C^1), 65.3 (d, C^2), 128.8–139.9 (m, MeC$_6$H$_4$), 128.3–137.1 (m, Ph), $^1J(^{13}C^1-^{103}Rh) = 12.4$ Hz, $^1J(^{13}C^2-^{103}Rh) = 10.3$ MHz. ^{29}Si{^{1}H}-NMR (C_7D_8, 298 K, 99.4 MHz) δ −11.9 (dd), $^3J(^{29}Si-^{31}P) = 1.7$ Hz, $^2J(^{29}Si-^{103}Rh) = 1.8$ Hz. ^{31}P{^{1}H}-NMR (C_7D_8, 298 K, 101 MHz): δ 49.7 (d), $^1J(^{31}P-^{103}Rh) =$ 179 Hz.

3.7. Synthesis of [{Rh(Vi$_2$SiMe$_2$)(μ-Cl)}$_2$] (7)

Divinyldimethylsilane (0.5 ml) was added to a rapidly stirring suspension of [{Rh(C_2H_4)$_2$(μ-Cl)}$_2$] (0.17 g, 0.44 mmol) in toluene (5 ml). The reaction mixture was allowed to stir for 3 h. The solvent and ethylene were removed under reduced pressure. The residual orange–red solid was dissolved in toluene (5 ml), filtered through Celite and washed with toluene (5 ml). The combined filtrate and washings were concentrated under reduced pressure to ca. 2 ml and stored at −30°C for 48 h, to yield orange red crystals of **7** (0.14 g, 0.28 mmol, 64%), m.p. 96–98°C. X-ray quality crystals were grown from *n*-pentane.

Anal. Found: C, 28.8; H, 4.8. $C_{12}H_{24}Cl_2Rh_2Si_2$. Calc. C, 28.8; H, 4.8%. ^{1}H-NMR (C_7D_8, 298 K, 500 MHz): δ −0.37 (s, Me_e, 3H), 0.54 (s, Me_a, 3H), 2.58 (m, H^3, 2H), 3.24 (dd, H^1, 2H), 3.58 (m, H^2, 2H), $^3J(^1H^1-^1H^2) = 11.2$ Hz, $^3J(^1H^1-^1H^3) = 15.4$ Hz, $^2J(^1H^2-^{103}Rh) = 1.4$ Hz, $^2J(^1H^3-^{103}Rh) = 1.3$ Hz. $^{13}C\{^1H\}$-NMR (C_7D_8, 313 K, 125.8 MHz): δ 1.2 (s, Me_e), 6.3 (s, Me_a), 57.2 (s, C_1), 72.0 (d, C_2), $^1J(^{13}C^2-^{103}Rh) = 14.0$ Hz. $^{29}Si\{^1H\}$-NMR (C_7D_8, 298 K, 99.4 MHz): δ −4.2 (s).

Table 3
Bond lengths (Å) and angles (°) for [(Rh(CH_2=CH)$_2$SiMe$_2$(μ-Cl)}$_2$] (**7**) [a]

Bond lengths (Å)			
Rh(1)–Cl(1)	2.389(2)	Rh(1)–Cl(2)	2.376(2)
Rh(1)–M(2)	2.024(9)	Rh(1)–M(1)	2.026(10)
Rh(1)–C(1)	2.146(8)	Rh(1)–C(2)	2.134(10)
Rh(1)–C(3)	2.141(8)	Rh(1)–C(4)	2.135(9)
Rh(2)–Cl(1)	2.385(2)	Rh(2)–Cl(2)	2.385(2)
Rh(2)–M(3)	2.019(9)	Rh(2)–M(4)	2.020(9)
Rh(2)–C(7)	2.145(8)	Rh(2)–C(8)	2.123(9)
Rh(2)–C(9)	2.135(8)	Rh(2)–C(10)	2.135(9)
Rh(1)···Rh(2)	3.133(1)	Si(1)–C(6)	1.847(8)
Si(1)–C(3)	1.852(9)	Si(1)–C(5)	1.856(8)
Si(1)–C(1)	1.867(8)	Si(2)–C(12)	1.850(8)
Si(2)–C(11)	1.850(9)	Si(2)–C(7)	1.850(9)
Si(2)–C(9)	1.865(9)	C(1)–C(2)	1.384(12)
C(3)–C(4)	1.381(19)	C(7)–C(8)	1.387(12)
C(9)–C(10)	1.380(19)		
Bond angles (°)			
M(2)–Rh(1)–M(1)	89.1(3)	M(2)–Rh(1)–Cl(2)	92.5(3)
M(1)–Rh(1)–Cl(2)	175.4(3)	M(2)–Rh(1)–Cl(1)	177.9(3)
M(1)–Rh(1)–Cl(1)	92.7(3)	Cl(2)–Rh(1)–Cl(1)	85.69(8)
M(3)–Rh(2)–M(4)	89.6(3)	M(3)–Rh(2)–Cl(9)	177.7(3)
M(4)–Rh(2)–Cl(2)	92.2(3)	M(3)–Rh(2)–Cl(1)	92.7(3)
M(4)–Rh(2)–Cl(1)	175.1(3)	Cl(2)–Rh(2)–Cl(1)	85.59(8)
Rh(2)–Cl(1)–Rh(1)	82.03(7)	Rh(1)–Cl(2)–Rh(2)	82.31(7)
C(6)–Si(1)–C(3)	116.2(4)	C(6)–Si(1)–C(5)	111.1(4)
C(3)–Si(1)–C(5)	109.1(4)	C(6)–Si(1)–C(1)	116.1(4)
C(3)–Si(1)–C(1)	94.3(4)	C(5)–Si(1)–C(1)	108.8(4)
C(12)–Si(2)–C(11)	109.8(4)	C(12)–Si(2)–C(7)	115.9(4)
C(11)–Si(2)–C(7)	111.3(4)	C(12)–Si(2)–C(9)	113.9(4)
C(11)–Si(2)–C(9)	111.7(4)	C(7)–Si(2)–C(9)	93.4(7)
C(2)–C(1)–Si(1)	124.7(7)	C(4)–C(3)–Si(19)	194.5(7)
C(8)–C(7)–Si(2)	121.6(7)	C(10)–C(9)–Si(2)	191.0(7)

[a] M1, M2, M3 and M4 are the midpoints of the C(1)–C(2), C(3)–C(4), C(7)–C(8) and C(9)–C(10) bonds, respectively.

Table 4
Crystal data and structural refinement parameters for **1**, **2** and **7**

	1	**2**	**7**
Formula	$C_{16}H_{36}Cl_2O_2Rh_2Si_4$	$C_{56}H_{52}Cl_2O_2Rh_2Si_4$	$C_{12}H_{24}Cl_2Rh_2Si_2$
M	649.5	1146.1	501.2
Crystal system	Triclinic	Monoclinic	Monoclinic
a (Å)	6.417(2)	15.118(5)	10.486(3)
b (Å)	8.290(4)	16.305(5)	14.339(3)
c (Å)	13.197(3)	21.784(6)	12.202(2)
α (°)	72.91(3)		
β (°)	86.94(2)	107.30(3)	90.30(2)
γ (°)	78.52(2)		
U (Å^3)	656.9	5125.3	1834.7
Z	1	4	4
$D_{calc.}$ (g cm^{-3})	1.64	1.48	1.82
Space group	$P\bar{1}$ (no. 2)	$P2_1/c$	$P2_1/c$ (no. 14)
θ_{max} for data collection (°)	25	25	
Unique reflections	9308	6080	3226
Reflections with $I>2\sigma(I)$	1898	4828	1991
R_1 [for $I>2\sigma(I)$]	0.039	0.085	0.044
wR_2 (for all data)	0.04	0.2159	0.086

3.8. X-ray structure determinations for *1*, *2* and *7*

Intensities were measured on an Enraf–Nonius CAD 4 diffractometer (**1** and **7**) or a Mar Research Image Plate system for **2** at 293 K with monochromatic Mo–K_α radiation ($\lambda = 0.71071$ Å). Corrections for absorption were applied using DIFABS for **1** and using psi-scan measurements for **2** and **7**. Refinement was by full-matrix least-squares on F, using Enraf–Nonius MOLEN programs for **1** and on F^2 using all reflections and SHELX-93 for **2** and **7**. Non-hydrogen atoms were refined anisotropically. For **1**, hydrogen atoms were fixed at calculated positions, except for the vinyl H atoms which were freely refined. For **2** and **7**, H atoms were included in riding mode (Table 4).

Acknowledgements

We thank the EPSRC and Dow Corning Ltd. (Barry) for the awards of CASE studentships to C. MacBeath and N.J.W. Warhurst and Dr Peter Hupfield for his interest and encouragement.

References

[1] (a) J.L. Speier, D.E. Hook (Dow Corning Corp.), US Patent No. 2 823 218 (1958); Chem. Abstr. 53 (1959) 16965. (b) J.L. Speier, J.A. Webster, G.H. Barnes, J. Am. Chem. Soc. 79 (1957) 974.

[2] (a) D.N. Willing, US Patent No. 3, 491, 593 (1968). (b) B.D. Karstedt, US Patent No. 3, 775, 452 (1973).

[3] G. Chandra, P.B. Hitchcock, M.F. Lappert, P.Y. Lo, Organometallics 6 (1987) 191.

[4] (a) P.B. Hitchcock, M.F. Lappert, N.J.W. Warhurst, Angew. Chem. Int. Ed. Engl. 30 (1991) 438. (b) M.F. Lappert, F.P.E. Scott, J. Organomet. Chem. 492 (1995) C11.

[5] P.B. Hitchcock, M.F. Lappert, C. MacBeath, F.P.E. Scott, N.J. Warhurst, J. Organomet. Chem. 528 (1997) 139.

[6] P.B. Hitchcock, M.F. Lappert, C. MacBeath, F.P.E. Scott, N.J.W. Warhurst, J. Organomet. Chem. 534 (1997) 139.

[7] G. Beuter, O. Heyke, I.P. Lorenz, Z. Naturforsch. 46b (1991) 1694.

[8] F.G.N. Cloke, P.B. Hitchcock, M.F. Lappert, C. MacBeath, G.O. Mepsted, J. Chem. Soc. Chem. Commun. (1995) 87.

[9] S.S.D. Brown, S.N. Heaton, M.H. Moore, R.N. Perutz, G. Wilson, Organometallics 15 (1996) 1392.

[10] J.W. Fitch, W.T. Osterloh, J. Organomet. Chem. 213 (1981) 493.

[11] A.R. Bassindale, S.S.D. Brown, P. Lo, Organometallics 13 (1994) 738.

[12] A.G. Avent, M.F. Lappert, C. MacBeath, J. Organomet. Chem. 502 (1995) 163.

[13] J.A. Ibers, R.G. Snyder, J. Am. Chem. Soc. 84 (1962) 495.

[14] R. Cramer, Inorg. Chem. 1 (1962) 722.

[15] R.B. King, Inorg. Chem. 2 (1963) 528.